the plant journal

SEB SOCIETY FOR EXPERIMENTAL BIOLOGY

The Plant Journal (2008) **55**, 89–103 doi: 10.1111/j.1365-313X.2008.03489.x

Altered plastid levels and potential for improved fruit nutrient content by downregulation of the tomato DDB1-interacting protein CUL4

Songhu Wang[1], Jikai Liu[1], Yuanyuan Feng[1], Xiangli Niu[1], Jim Giovannoni[2] and Yongsheng Liu[1,3,*]

[1]*Ministry of Education Key Laboratory for Bio-resource and Eco-environment, College of Life Science and State Key Laboratory of Hydraulics and Mountain River Engineering, Sichuan University, Chengdu 610064, China,*

[2]*US Department of Agriculture – Agricultural Research Service, Robert Holly Center and Boyce Thompson Institute for Plant Research, Cornell University, Ithaca, NY 14853, USA, and*

[3]*College of Life Science and Engineering, Southwest University of Science and Technology, Mianyang 621002, China*

Received 12 January 2008; revised 27 February 2008; accepted 5 March 2008; published online 21 May 2008.

[*]For correspondence (fax +86 28 8541 5300; e-mail liuyongsheng1122@yahoo.com.cn).

Summary

Fruits are a major source of nutrition in human diets, providing carbohydrates, fiber, vitamins and phytonutrients. Carotenoids are a principal class of compounds found in many fruits, providing nutritional benefits both as precursors to essential vitamins and as antioxidants. Molecular characterization revealed that the tomato *high pigment* mutant genes (*hp1* and *hp2*) encode UV-DAMAGED DNA BINDING PROTEIN-1 (DDB1) and DE-ETIOLATED-1 (DET1) homologs, respectively, and both are essential components of the recently identified CUL4-based E3 ligase complex. Here we have isolated a tomato CUL4 homolog and performed yeast two-hybrid assays to suggest possible association of tomato DDB1 with CUL4 and DET1. Real-time RT-PCR analysis indicated that both *HP1* and *CUL4* are expressed constitutively. Abscisic acid is implicated in plastid division control and its application substantially enhances *HP1/DDB1* mRNA accumulation. Transformation of constructs expressing CUL4–YFP and DDB1–YFP fusion proteins driven by the CaMV 35S promoter reveals that both CUL4 and DDB1 are targeted to tomato plastids and nuclei simultaneously. Using fruit-specific promoters combined with RNAi technology, we show that downregulated *DDB1* expression in transgenic fruits results in a significant increase in the number of plastids and corresponding enhanced pigment accumulation. CUL4-RNAi repression lines provide insight regarding CUL4 function during tomato development, and reveal that this tomato cullin is important in the regulation of plastid number and pigmentation, which in turn have a direct impact on fruit nutrient quality.

Keywords: fruit quality, DDB1, cullin4, plastid division, carotenogenesis, tomato.

Introduction

The fleshy fruit ripening-associated color development in many species is largely dependent on the differentiation and function of carotenoid-rich chromoplasts, a specialized organelle derived from plastids. One of the best-characterized genetic and molecular systems of carotenogenesis and fruit pigmentation is tomato (*Solanum lycopersicum*). The major pigments of ripe tomato fruit are carotenoids, specifically β-carotene and lycopene. β-carotene is a pro-vitamin A compound, and lycopene has been associated through epidemiological studies with a reduced incidence of degenerative diseases, including heart disease and cancer (Bendich, 1991; Hwang and Bowen, 2002).

In plants, an integral part of plastid development is division, as these organelles are not created *de novo* but arise by division through binary fission from pre-existing plastids in the cytosol. Plastid division in higher plants is a complex process that combines mechanisms of organelle constriction with assembly and expansion of membrane networks (Maple and Møller, 2007). Although progress has been made in defining some important components that function in the plastid division process, little is known about

the mechanisms that regulate total plastid volume within the cell. The strict maintenance of plastid populations in dividing cells and the alteration of plastid number and function in response to internal and external signals suggest coordinated cellular regulation of the plastid division process (Galpaz *et al.*, 2008; Jones *et al.*, 2002; Raynaud *et al.*, 2005).

Phytohormones and/or their signaling components functioning in plastid division and development have been documented. It has recently been reported that abscisic acid deficiency in the tomato mutant *high pigment 3* (*hp3*) leads to increased plastid number and higher fruit lycopene content (Galpaz *et al.*, 2008). A developmentally regulated (DR), nuclear-localized gene in tomato (DR12), a member of the auxin response factor (ARF) family, has been shown to regulate cell division and plastid division simultaneously (Jones *et al.*, 2002). Another molecular component linking the cell and plastid division cycles is Arabidopsis CDT1, a cyclin-dependent kinase that forms part of the pre-replication complex (Raynaud *et al.*, 2005).

In tomato, mutants with exaggerated photoresponsiveness and elevated pigmentation such as the *high pigment* mutants *hp1* and *hp2* have been identified (Kendrick *et al.*, 1997). Cloning the HP1 gene revealed that it encodes a protein homologous to UV-DAMAGED DNA BINDING PROTEIN-1 (*DDB1*) (Lieberman *et al.*, 2004; Liu *et al.*, 2004) and an Arabidopsis counterpart, *DDB1a*, whose product has been shown to interact with DE-ETIOLATED-1 (*DET1*) both biochemically and genetically (Schroeder *et al.*, 2002). DET1 was first identified in Arabidopsis as a negative regulator of photomorphogenic responses (Pepper *et al.*, 1994), and its tomato homolog HIGH PIGMENT-2 (HP2) has been implicated in negatively regulating fruit, leaf and seedling pigmentation (Davuluri *et al.*, 2004, 2005; Mustilli *et al.*, 1999). Extensive molecular and microscope analyses demonstrated that, in fully expanded leaf and/or fruit pericarp cells of *hp* mutants, there is increased chloroplast number and increased chloroplast size, suggesting a distinct function of HP1 and HP2 proteins in plastid division and development (Cookson *et al.*, 2003; Kolotilin *et al.*, 2007; Yen *et al.*, 1997).

Recently, two extensive studies in Arabidopsis have shown that DDB1a and DET1 together form a complex with Cullin4 (CUL4), an ubiquitin-conjugating E3 ligase, to target proteins for proteolysis (Bernhardt *et al.*, 2006; Chen *et al.*, 2006). Cullins are well-known central scaffolding subunits in eukaryotic E3 ligases that facilitate the ubiquitination of target proteins (for reviews, see Schwechheimer and Villalobos, 2004; Smalle and Vierstra, 2004). CUL4 has been highly conserved during evolution. Several studies have indicated an essential function for CUL4 in cell-cycle control, genomic stability and development (Bernhardt *et al.*, 2006; Chen *et al.*, 2006; Li *et al.*, 2002; Osaka *et al.*, 2000; Zhong *et al.*, 2003). Although both HP1/DDB1 and HP2/DET1, the Arabidopsis counterparts of DDB1a and DET1 respectively, have been implicated as major regulators of plastid phenotypes in tomato, the function of tomato *Cul4* remains largely unknown. The unique biology and activities of plastids in developing fleshy fruit warrants investigation of *Cul4* in these tissues. Here we show that tomato HP1 can directly interact with CUL4 and HP2 *in vitro*, respectively, and both HP1 and CUL4 proteins are targeted to nuclei and plastids simultaneously. Real-time RT-PCR analysis revealed that both *HP1* and *CUL4* are expressed constitutively, and abscisic acid (ABA) application substantially enhanced *HP1/DDB1* mRNA accumulation. Using fruit-specific promoters combined with RNAi, we show that directed repression of DDB1/HP1 expression in fruit tissue results in elevated pigment accumulation by increasing plastid compartment space. We also show that constitutive downregulation of tomato *Cul4* yields a pleiotropic phenotype, including developmental alteration, photomorphogenesis and enhanced pigmentation.

Results

Tomato CUL4 associates with HP1/HP2 in the yeast two-hybrid system

Tomato *Cul4* was isolated by RT-PCR using primers designed to published cDNA sequences (accession numbers Y16124 and BG131979), and the cloned cDNA was designated EU218537. Sequence analysis revealed that tomato CUL4 is a protein of 785 amino acids with a predicted molecular weight of 90 kDa. CUL4 contains a conserved cullin domain from amino acids 89–687. The C-terminal region from amino acids 706–785 encodes a highly conserved domain Pfam-B_851, which exists in almost all cullins although its function remains unknown (http://www.sanger.ac.uk/Software/Pfam). Protein alignment showed that tomato CUL4 is considerably more homologous to Arabidopsis CUL4 (81%) than to human CUL4a (46%; Figure S1).

To investigate whether HP1 (DDB1) and HP2 (DET1) interact with each other directly, or whether this interaction requires additional factor, we examined the interactions of tomato CUL4 with these two proteins by a directed yeast two-hybrid analysis. As shown in Figure 1, HP1 is capable of interacting with both tomato CUL4 and HP2, but no significant HP2–CUL4 interaction was detected, supporting the possible formation of the predicted CUL4–DDB1–DET1 complex.

Both tomato CUL4 and HP1 are expressed constitutively and targeted to nuclei and plastids simultaneously

To determine the expression patterns of tomato *Cul4* and *HP1/DDB1*, total RNAs were extracted from seedling roots, seedling stems, seedling leaves, flowers and fruit pericarp at various developmental stages. mRNA levels were analyzed by real-time RT-PCR. The results showed that tomato *Cul4*

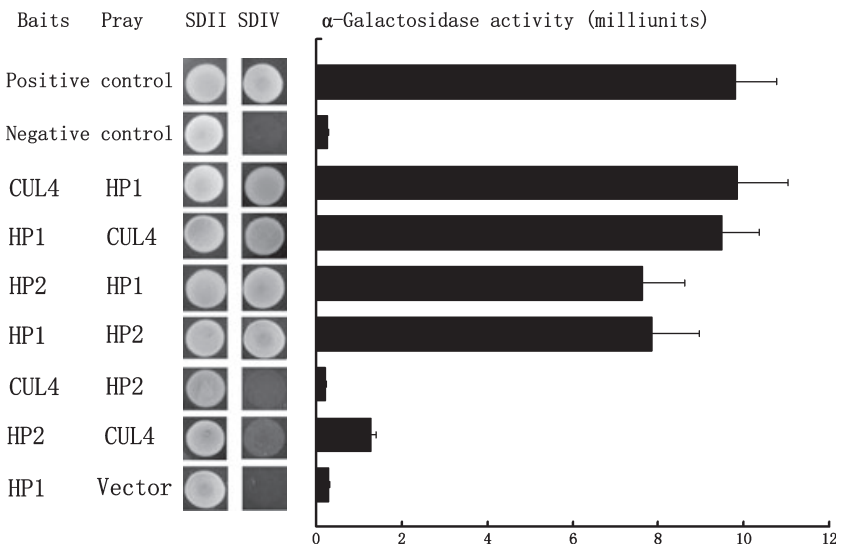

Figure 1. The interaction between tomato CUL4, HP1 and HP2 examined by yeast two-hybrid analysis.
SDII, selection medium for transformation with bait and prey plasmids supplemented with leucine and histidine; SDIV, selection medium for interaction studies without leucine and histidine supplements. Images were taken of single spots. The positive control was co-transformed using bait plasmid pGBKT7-53 (encoding a fusion between the GAL4 BD domain and murine p53) and prey plasmid pGADT7-T (encoding a fusion between GAL4 AD and the SV40 large T-antigen). The negative control comprised pGBKT7-Lam (encoding a fusion between GAL4 BD and human lamin C) and pGADT7-T. The α-galactosidase activities of co-transformed yeasts are shown. The results shown represent the mean values of 12 independent α-galactosidase assays, and the error bars represent SE.

and *HP1/DDB1* are expressed constitutively, both with apparently higher expression levels in flowers and with reduced levels following the onset of ripening (Figure 2a). In addition, real-time RT-PCR analysis was also used to determine tomato *Cul4* and *HP1/DDB1* mRNA levels in 10-day-old seedlings under various growth conditions. Interestingly, light intensity and application of indole-3-acetic acid (IAA) did not significantly alter the expression levels of either tomato *Cul4* or *HP1/DDB1*, but application of abscisic acid (ABA) substantially enhanced *HP1/DDB1* mRNA accumulation (Figure 2b).

The subcellular localization of tomato CUL4 and HP1 were determined in transgenic plants expressing either CUL4 or HP1 fused to YFP. Both CUL4 (Figure 2e,f) and HP1 (Figure 2h,i) are targeted to nuclei and plastids, and were observed simultaneously in both organelles. By contrast, YFP alone is not targeted to either nuclei or plastids and is evenly distributed in the cytoplasm (Figure 2g). Substantial autofluorescence was exclusively observed in the cell wall in both transgenic plants (Figure 2e,g,h) and the wild-type controls, but not in control nuclei or plastids (Figure 2c,d).

Directed disruption of HP1/DDB1 in fruit tissues phenocopies HP1 mutant fruit

Spontaneous and induced mutations at the *HP1/DDB1* locus show developmental defects such as reduced plant stature and fruit yield in addition to elevated plastid number (Kendrick *et al.*, 1997). To exploit the positive effects of *DDB1/HP1* gene inhibition in fruits without the deleterious developmental effects on plant growth and development, we suppressed *DDB1*/*HP1* expression through RNAi specifically in fruits, using *DDB1*/*HP1*-derived inverted-repeat constructs driven by one of two fruit-specific promoters, 2A11 and TMF7 (Pear *et al.*, 1989; Santino *et al.*, 1997). Constructs were introduced into normal tomatoes by *Agrobacterium*-mediated T-DNA transfer. We generated a number of transgenic plants that contain each of these constructs manifesting normal and healthy vegetative growth, but setting darker green immature fruits (Figure 3a–c) and reminiscent of *hp1* mutant fruits (Kendrick *et al.*, 1997). While the green fruit phenotype is easily observed, color differences in ripe fruit are more difficult to detect visually but are readily observed via HPLC analysis (Kendrick *et al.*, 1997; Liu *et al.*, 2004). Immature fruits of plants containing the TMF7 construct (Figure 3b) were generally darker than the fruits of transgenic plants containing the 2A11-driven promoter construct (Figure 3c). In T_1 segregating populations, we observed a correlation of transgene integration with progeny having dark-green immature fruits, for both constructs (data not shown).

The fruit-specific phenotypes of transgenic plants containing fruit-driven promoter constructs suggested that *HP1/DDB1* gene expression had been silenced. To ensure that observed phenotypes correlated with reduced transcripts, we examined endogenous *HP1/DDB1* mRNA abundance in the transgenic plants using real-time quantitative RT-PCR, as previous efforts suggested that *HP1/DDB1* transcripts were difficult to detect by RNA gel blotting (Y.L. and J.G., unpublished data). Total RNA was harvested from leaves and immature fruits derived from three independent primary transformants containing each construct. Analysis of the real-time RT-PCR results indicated a substantial reduction in endogenous *HP1/DDB1* transcript levels specifically in the fruit tissue of transformants as compared to wild-type fruits, whereas in RNA extracted from leaves there was no significant difference in the abundance of *HP1/DDB1* mRNA between transgenic and wild-type plants (Figure 4a). Similar results were shown for both fruit-specific promoter constructs

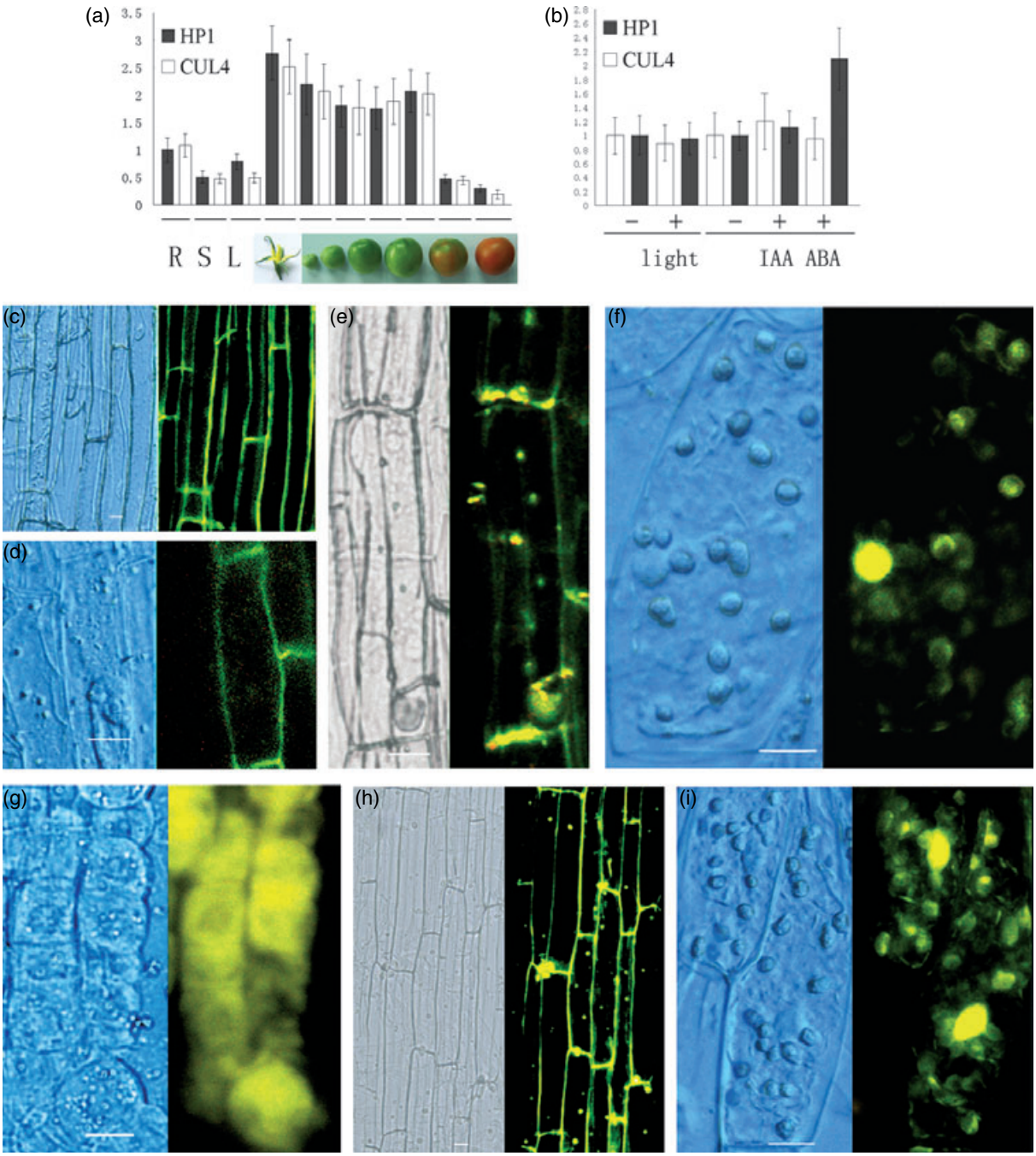

Figure 2. Expression patterns and subcellular localizations of tomato CUL4 and HP1.
The mRNA levels for tomato *Cul4* and *HP1* were analyzed by real-time quantitative RT-PCR.
(a) Constitutive expression of tomato *Cul4* and *HP1* in various tissues. Total RNAs were extracted from roots (lane R), stems (lane S), leaves (lane L), flowers and fruit pericarps at various developmental stages [10, 15, 20 and 25 days post-anthesis, breaker and ripe, respectively). (b) Expression patterns of tomato CUL4 and HP1 in seedlings grown under various conditions. Total RNAs were extracted from 10-day-old seedlings under the growth conditions of light (+) or darkness (–), and with application of indole-3-acetic acid (IAA) or abscisic acid (ABA). (c–i) Tomato CUL4 and HP1 targeting to both the nucleus and plastids. The left panels show images from differential interference contrast (DIC) and the right panels show the corresponding fluorescent images. Bars = 10 μm. (c, d) Root cells from wild-type seedling (c) and callus (d), showing autofluorescence from the cell wall. The exposure time was 900 msec. (e, f) CUL4 protein targeting to both nuclei and plastids in root cells prepared from 35S-CUL4-YFP transgenic tomato callus. The exposure time was 400 msec. (g) YFP protein is evenly distributed in cytoplasm of root cells prepared from 35S-YFP transgenic tomato callus. The exposure time was 450 msec. (h, i) HP1 protein accumulation in both nuclei and plastids of root cells prepared from 35S-HP1-YFP transgenic tomato callus. The exposure time was 400 msec.

(Figure 4a). This was in contrast to results for non-transformed plants.

Constitutive downregulation of tomato Cul4 *results in pleiotropic phenotypes including dark-green immature and subsequently dark-red ripening fruits*

To further address the functional significance of the tomato *Cul4*-encoded protein and to explore its physiological role, transgenic tomato lines were generated expressing tomato *Cul4*-derived inverted-repeat sequences under the direction of the 35S promoter. Primary transgenics (T_0) resulted in PCR amplification with primers designed to the *NPTII* (kanamycin resistance) marker. In T_1-segregating populations, we observed a correlation of transgene integration with inverted-repeat *Cul4* progeny having dark-green immature fruits and leaves compared with both progeny segregating out the transgene and normal plants (Figure 3). To ensure that observed phenotypes correlated with the downregulated transcript, we investigated endogenous *Cul4* mRNA levels in the transgenic plants using real-time quantitative RT-PCR. Total RNA was extracted from leaves and immature fruits of transgenic and non-transgenic plants segregated out from three independent CUL4-RNAi repression lines. Analysis of real-time quantitative RT-PCR revealed a distinct reduction in endogenous *Cul4* transcript levels in CUL4-RNAi repression lines compared to that of non-transgenic and wild-type plants (Figure 4b).

To obain information about the function of tomato *Cul4* during plant development, three CUL4-RNAi repression lines corresponding to independent transformation events and showing notable phenotypic effects were selected for further molecular and phenotypic characterization. As shown in Figure 3, similar to the *hp1* mutant, in addition to the dark-green immature fruits and leaves, the most visible effects of downregulated *Cul4* expression on plant development included inhibited plant stature or dwarfing (Figure 3f). A unique phenotype resulting from tomato CUL4 deficiency includes a reduction of floral and fruit size (Figure 3e,i and Table 1). Detailed phenotypic analyses of the CUL4-RNAi repression lines revealed that an approximately 50% reduction of internode length accounts for the decrease in plant stature (Figure 5). Reduced tomato *Cul4* expression also leads to an approximate 100% increase of trichome abundance on leaves, while the spontaneous *hp1* mutant shows similar trichome abundance compared to the wild-type control (Figure 3l and Table 1). In addition, strong reduction of tomato *Cul4* expression results in split sepals and petals, as indicated by the increased number of sepals and petals in each floral organ (Figure 3i,j and Table 1).

Because tomato CUL4 associates with HP1/DDB1 and HP2/TDET1, we speculated that tomato *Cul4* repression lines might display defects in photomorphogenesis, as has been described for *hp* mutants showing hypersensitive photomorphogenic responsiveness (Kendrick *et al.*, 1997; Liu *et al.*, 2004; Mustilli *et al.*, 1999). To identify defects in the photomorphogenic response, three independent CUL4-RNAi repression lines, *hp1* and wild-type seedlings were cultured for 7 days in white light (16 h light, 8 h dark) or in complete darkness. We did not detect any major changes in the formation of the apical hook or cotyledons. However, under light-grown conditions, both *hp1* and downregulated *Cul4* transgenic seedlings developed reduced hypocotyls in comparison with wild-type plants (Figures 3g and 5), while the difference in hypocotyl length between dark-grown functionally deficient and wild-type seedlings is not as obvious as that observed in the light-grown seedlings (Figure 5). Also, the transcription of two light-responsive genes (*CHS* and *CAB*) in both *hp1* and downregulated *Cul4* transgenic seedlings was detectable by RT-PCR in darkness and greatly enhanced by light compared to the controls (Figure 3h). A previous study demonstrated that, when seedlings were harvested in complete darkness, the *hp1* mutation resulted in significant *CAB* mRNA accumulation (Peters *et al.*, 1998). These findings suggest that both tomato CUL4 and HP1/DDB1 participate in some aspects of photomorphogenesis, including seedling hypocotyl elongation.

Inhibited Cul4 and HP1/DDB1 expression results in increased plastid compartment area

To investigate differences in chloroplast populations in mesophyll cells between CUL4-RNAi repression lines and wild-type controls, chloroplast numbers and sizes were determined in preparations of fixed isolated mesophyll cells from fully expanded leaves. In fully expanded leaves of *Cul4* repression lines and the spontaneous *hp1* mutant, chloroplast density (expressed as chloroplasts number per unit cell plan area) in both palisade and spongy mesophyll cells was found to be increased compared to wild-type (Figure 6a–f). This increased chloroplast number was found across the range of cell sizes in palisade cells (Figure 6g) and also in larger spongy mesophyll cells (Figure 6h) derived from the fully expanded leaves.

To compare plastid compartment sizes in fruit pericarp cells between wild-type and transgenic plants containing either the CaMV35S-CUL4-RNAi, 2A11-HP1-RNAi or TFM7-HP1-RNAi construct, pericarp cells were isolated from identical positions in mature green and red ripe fruits (Table 2). In all the lines tested, the plastid number per cell and plastid density did not change substantially within lines between the mature green and red ripe stages. A slight increase in plastid plan area and total plastid area per cell was noted. We observed significant variation in plastid number and plastid size among the various lines (Figure 7a–h). Pericarp cells in both mature green and red ripe fruits derived from transgenic plants containing either the CaMV35S-CUL4-RNAi, 2A11-HP1-RNAi or TFM7-HP1-RNAi construct showed

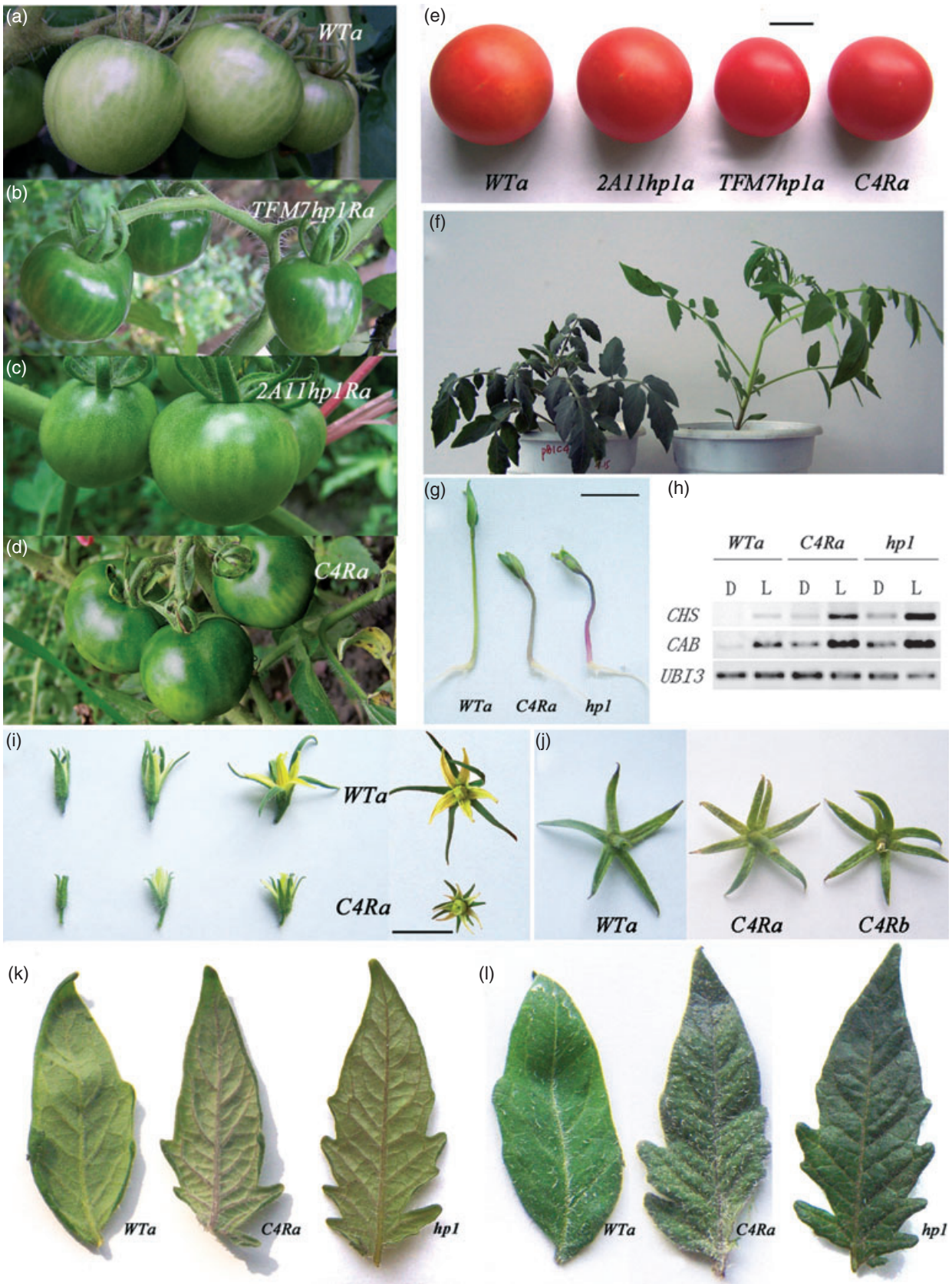

an increase in plastid number and plastid size compared to wild-type (Table 2).

RNAi repression plants exhibited elevated accumulation of carotenoids and flavanoids

Light-grown seedlings of 35S-CUL4-RNAi repression lines display elevated levels of anthocyanins, but these effects are not as severe as observed in the *hp1* mutant (Figure 3g). Increased anthocyanin accumulation in leaf veins was visible in 35S-CUL4-RNAi repression lines and the *hp1* mutant (Figure 3k), indicating that silencing of *Cul4* might enhance transcription of anthocyanin biosynthetic genes in such tissues. Indeed, real-time quantitative RT-PCR demonstrated that the transcription levels of two major genes of anthocyanin biosynthesis (*CHI*, chalcone isomerase; *CHS*, chalcone synthase) were elevated in the three CUL4-RNAi repression lines in addition to the original spontaneous *hp1* mutant, while expression levels of two major genes of carotenoid biosynthesis (*PSY2*, phytoene synthase 2; *PDS*, phytoene desaturase) were not significantly altered in these lines (Figure 8). Chemical analysis revealed that downregulation of *Cul4* expression increases anthocyanin and chlorophyll accumulation by 85–90% and 80–90%, respectively (Figure 9a,b).

We conducted HPLC analysis of carotenoids for three independent T_1 segregating populations derived from each of the 35S-CUL4-RNAi, 2A11-HP1-RNAi or TFM7-HP1-RNAi repression transformants. Samples from three or four ripe fruits from three sibling T_1 generation plants per line were subjected to HPLC analysis. Lycopene, β-carotene and total carotenoids were present at higher levels in transgenic fruits containing the three constructs (Figure 9c–e). The plants containing 35S-CUL4-RNAi and TFM7-HP1-RNAi showed up to twofold higher levels of lycopene, while 2A11-HP1-RNAi repression increased lycopene content by approximately 20% compared with normal controls (Figure 9d). β-carotene levels in fruits expressing all three constructs were higher than in wild-type fruits (Figure 9e).

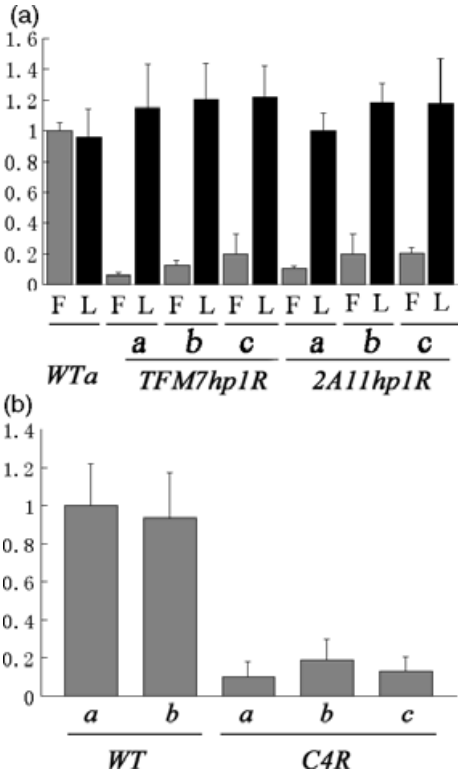

Figure 4. Analysis of tomato *Cul4* and *HP1* mRNA levels in transgenic plants.
R indicates the presence of the relevant RNAi construct.
(a) Real-time quantitative RT-PCR analysis of *HP1* mRNA levels in immature fruits 25 days post-anthesis (F) and fully expanded leaves (L) from wild-type Ailsa Craig (*WTa*) and three independent transgenic lines containing the fruit-specific promoters 2A11 (*2A11hp1Ra*, *b* and *c*) or TFM7 (*TFM7hp1Ra*, *b* and *c*). Each bar represents three repetitions from each RNA sample (derived from pools of three fruits or leaves per plant). Error bars representing standard errors are shown in each case.
(b) Real-time quantitative RT-PCR analysis of tomato *Cul4* mRNA levels in immature fruits 25 days post-anthesis from wild-type Ailsa Craig (*WTa* and *b*) and three independent CUL4-deficient lines (*C4Ra*, *b* and *c*) containing the 35S-CUL4-RNAi construct. Each bar represents three repetitions from each RNA sample (derived from pools of three fruits per plant). Error bars representing standard errors are shown in each case.

Figure 3. Normal, mutant and transgenic plant phenotypes.
R indicates the presence of the relevant RNAi construct.
(a–d) Representative immature fruits from field-grown plants of wild-type Ailsa Craig (*WTa*), HP1-deficient lines (*TFM7hp1Ra* and *2A11hp1Ra*) driven by fruit-specific promoters TFM7 and 2A11, and a CUL4-deficient line (*C4Ra*) driven by the 35S promoter, respectively.
(e) Representative red ripe fruits from field-grown plants of wild-type Ailsa Craig (*WTa*), HP1/DDB1-deficient lines driven by fruit-specific promoters 2A11 (*2A11hp1Ra*) and TFM7 (*TFM7hp1Ra*), and a CUL4-deficient line driven by the 35S promoter (*C4Ra*), respectively. Bar = 2 cm.
(f) Representative 30-day-old plants of a CUL4-deficient line (*C4Ra*) and wild-type Ailsa Craig (*WTa*) grown in the artificial climate incubator.
(g) Representative 7-day-old seedlings of wild-type Ailsa Craig (*WTa*), a CUL4-deficient line (*C4Ra*) and the *hp1* mutant germinated under white-light conditions with a 16 h light/8 h dark photoperiod. Bar = 1 cm.
(h) Semi-quantitative RT-PCR analysis of mRNA levels of light-regulated genes including *CAB* and *CHS*. Total RNAs were extracted from 7-day-old seedlings of wild-type Ailsa Craig (*WTa*), CUL4-deficient (*C4Ra*) and *hp1* mutant lines grown under complete darkness (D) or white-light (L) conditions with a 16 h light/8 h dark photoperiod.
(i) Comparison of flowers between wild-type Ailsa Craig (*WTa*) and a CUL4-deficient line (*C4Ra*), showing the variation in flower size and petal number. Bar = 2 cm.
(j) Comparison of sepal numbers between wild-type Ailsa Craig (*WTa*) and CUL4-deficient lines *C4Ra* and *C4Rb*. (k,l) Levels of anthocyanin accumulation and trichome growth in leaves from wild-type Ailsa Craig (*WTa*), a CUL4-deficient line (*C4Ra*) and *hp1* mutant plants. The plants were grown in the artificial climate incubator and harvested 30 days after germination.

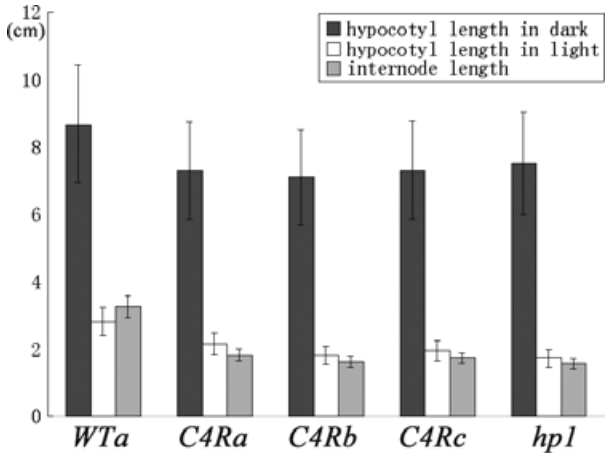

Figure 5. Quantification of tomato *Cul4* repression effects.
R indicates the presence of the relevant RNAi construct. Mean values of hypocotyl length from 20 seedlings grown at 25°C for 7 days in absolute darkness or under a 16 h light/8 h dark photoperiod are shown. Wild-type Ailsa Craig (*WTa*), three independent CUL4-deficient lines (*C4Ra*, *b* and *c*) and the *hp1* mutant were planted in artificial climate incubators and the internode length was measured 30 days after planting. Mean values of internode length from 10 repetitions of two sibling plants per line and standard errors are shown. Statistical analysis of differences in transgenic lines and *hp1* with respect to *WTa* was performed using Student's *t* test (*C4Ra*, *b*, *c*, $P < 0.001$; *hp1*, $P < 0.001$).

Discussion

The present investigation provides novel information about the function of tomato CUL4 and DDB1 (HP1) in fleshy fruit tissues that has not been not revealed in studies using the research model Arabidopsis. Yeast two-hybrid assays suggest possible association of HP1 with CUL4 and HP2. Transformation with CUL4–YFP and HP1–YFP fusion proteins driven by the 35S promoter demonstrated that both CUL4 and HP1 are simultaneously localized in nuclei and plastids. Using fruit-specific promoters combined with RNAi technology, fruit-specific downregulation of *HP1* expression resulted in an increase in plastid compartments and enhanced pigment accumulation in both immature and mature fruit tissues. In addition, the observed phenotypes of the 35S-CUL4-RNAi repression lines provide an indication of CUL4 function during tomato development, and reveal that this tomato cullin is important in regulation of plastid number and pigmentation.

Conserved from fission yeast to humans, the DDB1–CUL4 complex is a recently identified cullin-RING ubiquitin ligase that is involved in regulation of DNA replication, DNA repair and transcription, and can be subverted by pathogenic viruses to benefit viral infection (Angers *et al.*, 2006; Li *et al.*, 2006; Petroski and Deshaies, 2005). It has been proposed that DDB1 participates in targeting the substrate c-Jun to the CUL4–DDB1 E3 complex by interacting with an undefined motif present in the human DET1 protein (Wertz *et al.*, 2004). In Arabidopsis, DDB1a protein has been shown to interact with DET1 (Al Khateeb and Schroeder, 2007; Schroeder *et al.*, 2002), and CUL4 has been demonstrated to form an active E3 complex with DDB1a and DET1 to repress photomorphogenesis (Bernhardt *et al.*, 2006; Chen *et al.*, 2006). Viewed in the context of Arabidopsis data, it seems most plausible that the tomato CUL4, DDB1/HP1 and DET1/HP2 proteins are able to form a similar CUL4–HP1–HP2 complex and interact comparably to Arabidopsis CUL4, DDB1a and DET1. Notably, mutations in tomato DDB1 (*high pigment-1*) and tomato DET1 (*high pigment-2*) are responsible for *high pigment* phenotypes characterized by exaggerated photoresponsiveness and pigmentation. The *hp1 hp2* double mutant displays a synergistic phenotype, indicating association between tomato DET1 and DDB1 (Davuluri *et al.*, 2005; Lieberman *et al.*, 2004; Liu *et al.*, 2004; Mustilli *et al.*, 1999). Consistently, the data from yeast two-hybrid assays suggest

Table 1 Leaf trichome density and flower and fruit characterization

Line	Trichome density (number per cm^2)	No. flowers with various sepal numbers			No. flowers with various petal numbers				Size of flowers and fruit (cm)	
		Five	Six	Seven	Five	Six	Seven	Eight	Sepal length	Fruit transverse diameter
C4Ra	78 ± 6	0	14	18	0	21	9	2	0.9 ± 0.23	4.9 ± 0.30
C4Rb	80 ± 8	0	13	20	0	20	10	3	1.2 ± 0.34	4.7 ± 0.27
C4Rc	70 ± 6	0	16	16	0	20	11	1	1.3 ± 0.32	4.8 ± 0.28
hp1	40 ± 4	9	21	1	13	15	3	0	1.9 ± 0.23	5.8 ± 0.25
WTa	38 ± 5	27	36	2	27	33	5	0	2.0 ± 0.25	5.9 ± 0.30

Three independent CUL4-deficient lines (*C4Ra*, *b* and *c*), the *hp1* mutnat and wild-type Ailsa Craig (*WTa*) were included in the trichome abundance measurements and flower classification.
Young leaves at the same developmental stage were taken from 30-day-old plants grown in the artificial climate incubator, and trichome number was counted visually using a dissecting microscope. Trichome density was calculated as the trichome number per unit leaf area. Twenty leaves per line were observed and the mean values ± SE are shown.
Flowers were divided into various categories with individual sepal or petal numbers. Between 32 and 65 flowers per line were investigated.
Flowers at anthesis and red ripe fruits were used for measuring the organ size. Fifteen samples were observed, and the mean values ± SE are shown.

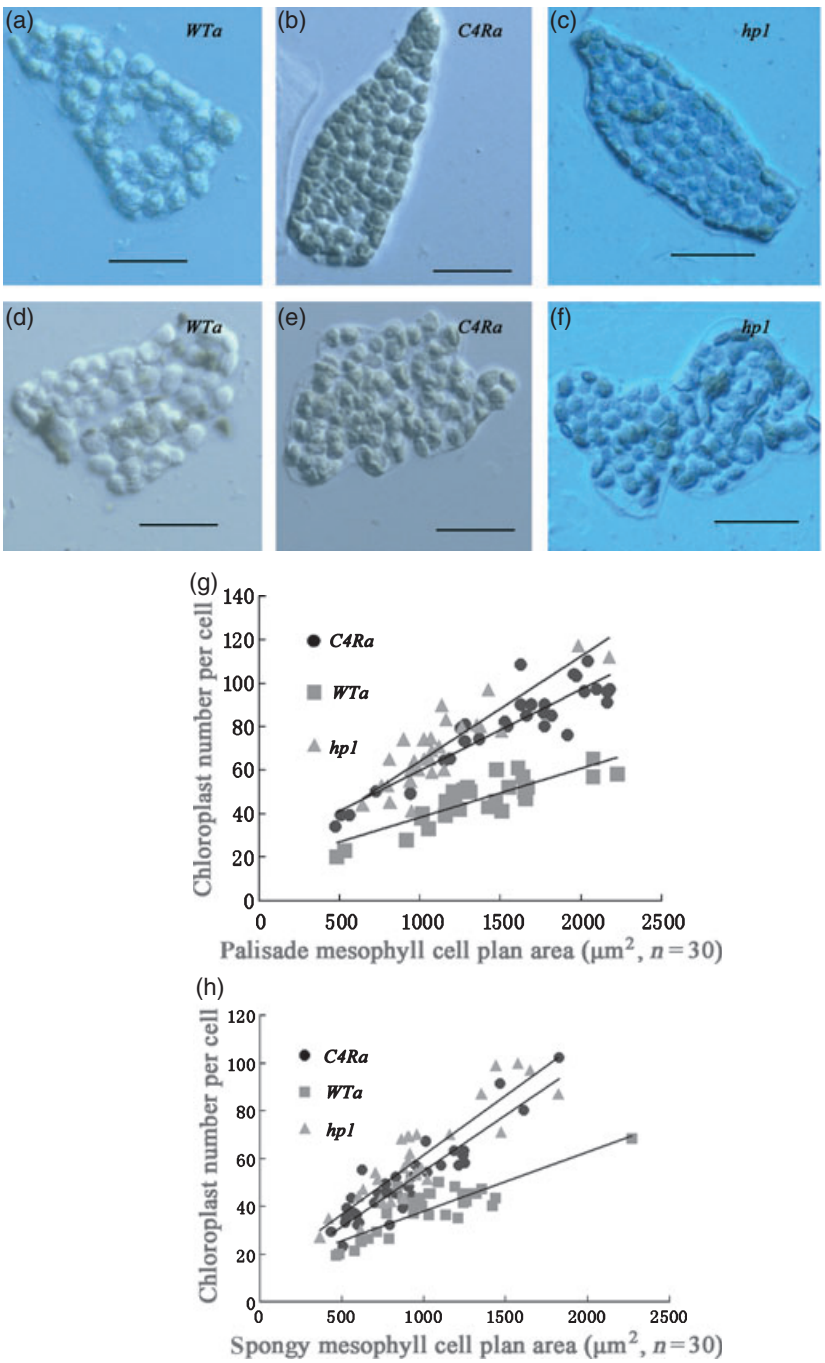

Figure 6. Alteration of plastid compartment size in leaf cells of transgenic plants.
Observations were carried out using differential interference contrast (DIC) optics on a Leica DMI6000B microscope. *R* indicates the presence of the relevant RNAi construct.
(a–c) Isolated palisade mesophyll cells from fully expanded leaves of wild-type Ailsa Craig *WTa* (a), CUL4-deficient line *C4Ra* (b) and the *hp1* mutant (c) grown in artificial climate incubators. Bars = 20 μm.
(d–f) Isolated spongy mesophyll cells from *WTa* (d), *C4Ra* (e) and *hp1* (f) grown in artificial climate incubators. Bars = 20 μm.
(g, h) Relationship between palisade mesophyll cell plan area and chloroplast number per cell (g) and spongy mesophyll cell plan area and chloroplast number per cell (h) for *WTa*, *C4Ra* and the *hp1* mutant.

that a CUL4–HP1–HP2 complex exists *in vivo* in tomato. Indeed, a number of studies have indicated that a direct protein–protein interaction between DDB1 (HP1) and CUL4 is highly conserved across animals and plants. In both humans and Arabidopsis, the N-terminal region of CUL4 and a central section of DDB1 are required for assembly of the two proteins, and the high level of conservation suggests that interaction of CUL4 with DDB1 (HP1) in tomato might be typical of previously described interactions between a cullin and its substrate adaptor protein for CUL4-based E3 ligase (Bernhardt *et al.*, 2006; Chen *et al.*, 2006; Figueroa *et al.*, 2005; Hu *et al.*, 2004; Jin *et al.*, 2006; Pintard *et al.*, 2003; Wertz *et al.*, 2004).

Microscopic observations and molecular analysis revealed a significant increase in chloroplast size and number in the *hp* mutants, and the elevated chloroplast area results in an increased sink size for pigment accumulation (Cookson *et al.*, 2003). Both constitutive co-suppression and specific downregulation at the tomato *DET1/HP2* locus result in pigment over-production (Davuluri *et al.*,

Table 2 Cell and plastid (chloroplast and chromoplast) characteristics of fruit pericarp cells from tomato cv. Ailsa Craig (*WTa*), CUL4-RNAi (*C4Ra*) and *HP1* fruit-specific RNAi transgenic plants activated by fruit-specific promoters (*2A11hp1Ra* and *TFM7hp1Ra*)

	WTa		*C4Ra*		*2A11hp1Ra*		*TFM7hp1Ra*	
	Mature green	Ripe	Mature green	Ripe	Mature green	Ripe	Mature green	Ripe
Cell plan area (μm^2, $n = 30$)	48 595 ± 2773	52 967 ± 2852	52 009 ± 3252	52 648 ± 2031	51 318 ± 2248	51 149 ± 2421	51 956 ± 3142	52 679 ± 2053
Plastid number per cell ($n = 30$)	548 ± 28	563 ± 31	718 ± 31	736 ± 26	661 ± 22	673 ± 26	703 ± 28	741 ± 28
Plastid density (per μm^2 cell plan area, $n = 30$)	0.011	0.0106	0.014	0.014	0.013	0.013	0.0135	0.014
Plastid plan area (μm^2, $n > 100$)	15.2 ± 0.3	16.8 ± 0.36	20.4 ± 0.35	24.4 ± 0.44	19.2 ± 0.34	22.1 ± 0.58	24.8 ± 0.32	29.8 ± 0.55
Total plastid area per cell (μm^2, $n = 30$)	8337 ± 431	9474 ± 519	14 650 ± 633	17 962 ± 645	12 689 ± 428	14 879 ± 590	17 444 ± 695	22 081 ± 848
Cell index	0.171	0.179	0.281	0.341	0.247	0.291	0.336	0.419

Values are means ± SE. Cell index is calculated as total plastid area per cell plan area. Mature green fruit were studied at 30 days post-anthesis; ripe fruit were studied at 9 days post-breaker.

2004, 2005). However, constitutive silencing by RNAi at the tomato *DDB1/HP1* locus did not yield viable plants (Y.L. and J.G., unpublished data), suggesting a fundamental function for DDB1 at early developmental stages of tomato. The current experiment demonstrated that fruit-specific silencing of *DDB1/HP1* leads to an elevated plastid compartment area. Furthermore, constitutive repression of tomato *Cul4* also increased plastid compartment space. These results suggest the negative nature of DDB1/HP1 and CUL4 as important components of an E3 complex involved in the regulation of plastid size and plastid number, and subsequently in enhancement of carotenoid accumulation in tomato fruits.

Similar to previous observations (Chen *et al.*, 2006; Ishibashi *et al.*, 2003), the present study reveals that both tomato CUL4 and DDB1/HP1 are predominantly localized in nuclei. Intriguingly, we also found that these proteins are abundant in plastids. The unique plastid localizations of these proteins appear to be consistent with the plastid phenotypes resulting from alteration of corresponding gene expression levels. These observations suggest a possible regulation of ubiquitin-mediated degradation in both organelles. One possible substrate of this complex is CDT1, a member of the pre-replication complex (Hu *et al.*, 2004). Arabidopsis CDT1a and CDT1b have been shown to localize simultaneously in nuclei and plastids, and their downregulation results in alteration of both nuclear DNA replication and plastid division (Raynaud *et al.*, 2005). Additionally, Arabidopsis CDT1a has been demonstrated to be degraded by the 26S proteasome (Castellano *et al.*, 2004). Comparably, human CUL4a and DDB1 proteins were observed simultaneously in cytoplasm and nucleus (Chen *et al.*, 2001), and degradation of human CDT1 has been linked to the function of CUL4a–DDB1 E3 ligase (Higa *et al.*, 2003; Hu *et al.*, 2004; Zhong *et al.*, 2003). However, the hypothesis that a CUL4–HP1 complex targets the tomato homolog of CDT1 for ubiquitin-conjugated proteolysis needs to be further elucidated once this gene is available.

Intriguingly, although accumulated biochemical evidence has indicated that CUL4 and DDB1/HP1 form a complex, some developmental alterations in the CUL4 RNAi repression lines do not occur in the *hp1* mutant background. One possible reason is that these two proteins are additionally involved in differential and independent cellular processes as implied by several studies (Cang *et al.*, 2006; Li *et al.*, 2006; Osaka *et al.*, 2000; Zhong *et al.*, 2003). In addition, even though several lines of evidence have now established a major role of DDB1 as a core subunit of the Cul4-based ubiquitin E3 ligase complex, DDB1 protein has been implicated in several other cellular functions, such as DNA repair activity (Sun *et al.*, 2002). It is noteworthy that point mutation is somewhat different from RNAi repression, and that the point mutation resulting in the high-pigment phenotype (*hp1*) does not necessarily abrogate the function of the HP1

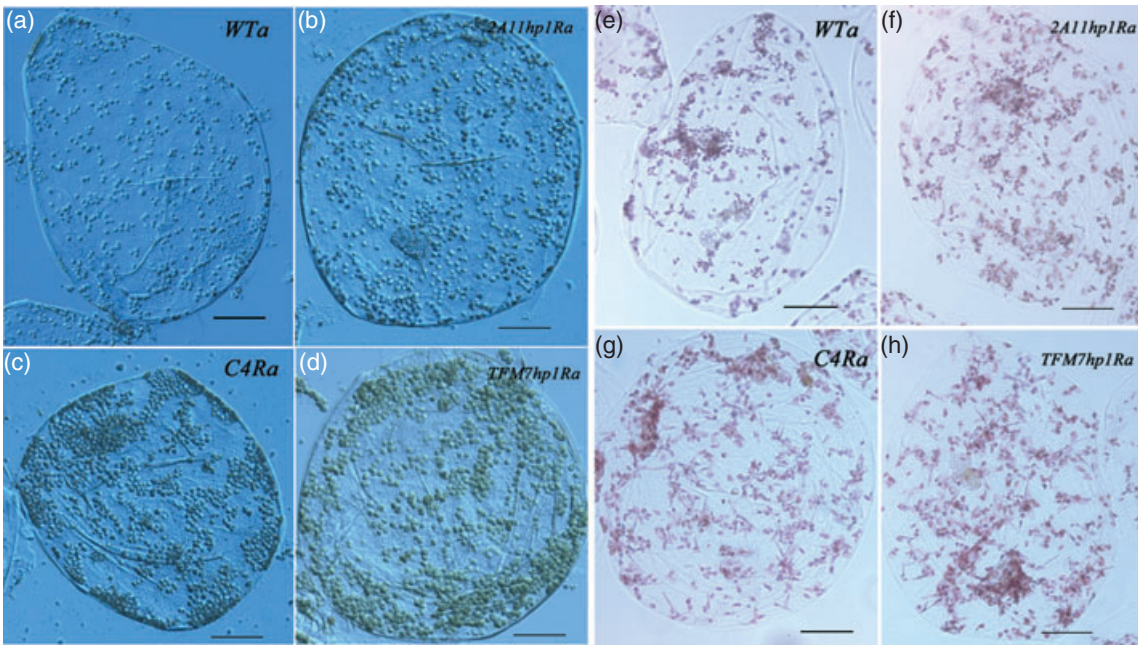

Figure 7. Alteration of plastid compartment size in pericarp cells of transgenic plants.
R indicates the presence of the relevant RNAi construct.
(a–d) Isolated pericarp cells from mature green tomato fruits of wild-type Ailsa Craig *WTa* (a), CUL4-deficient line *C4Ra* (c) and *hp1* fruit-specific promoter RNAi transgenic lines *2A11hp1Ra* (b) and *TFM7hp1Ra* (d). Bars = 50 μm.
(e–h) Isolated pericarp cells from fully ripe tomato fruits of *WTa* (e), *C4Ra* (g), *2A11hp1Ra* (f) and *TFM7hp1Ra* (h). Bars = 50 μm.

mutant protein completely. It is possible that the residual functions responsible for trichome or sepal development are retained in the mutant proteins.

Experimental procedures

Plant growth conditions

Tomato plants were germinated and grown in an artificial climate incubator (BINDER; http://www.binder-world.com) under standard conditions (26°C day, 18°C night; 16 h light, 8 h dark). Primary transformants (T_0) and transgenic generation 1 (T_1) plants were planted in the artificial climate incubators and transplanted into the field 35 days later. For hypocotyl measurements, T_2 populations and controls were germinated in water/agar in sterile jars under white light (16 h light, 8 h dark) or continuous darkness at 25°C. For plant hormone treatment, 10-day-old seedlings were harvested and incubated in 50% MS buffer with or without 20 μM IAA (or 2 mg l^{-1} ABA) for 3 h. Thereafter, seedlings were immediately frozen in liquid nitrogen and stored at −80°C until RNA extraction.

Plasmid construction and tomato transformation

DNA manipulations were carried out by using standard procedures (Sambrook and Russell, 2007). Sequences from *CUL4* cDNA (accession number EU218537) were amplified by RT-PCR for construction of the 35S-CUL4-RNAi vector. An inverted-repeat fragment was constructed in vector pSK int (Guo *et al.*, 2003) and transferred into PBI121 (driven by the 35S promoter) at the *Xba*I and *Sac*I restriction sites by PCR using primers CUL4Z-F (5′-AGAGAATTCGTGCTGGCAATAAAGGTA-3′), CUL4Z-R (5′-CTGCGAGCTCCTTTTTTCCTT-3′), CUL4F-F (5′-CGAGAAGCTTCGTGCTGGCAA-3′) and CUL4F-R (5′-TATCTCGAGTCTAGAACGCAGTGGCCCAATGAAT-3′), introducing unique restriction sites at the product ends. The resulting construct CaMV35S-CUL4-RNAi was created. Sequences from two fruit-specific promoters, 2A11 (accession number M87659; Pear *et al.*, 1989) and TFM7 (accession number X95261; Santino *et al.*, 1997), were amplified by PCR using primers 2A11-F1 (5′- GTGGGTCACAAGCTTGATACGTTATCA-3′), 2A11-R1 (CAGTCTAGATGGTTTTGGATTAATTGCTAA-3′), TFM-F1 (5′-TCTAAGCTTAATTAACTTGAT-TTTGAGTCCATG-3′) and TFM-R1 (5′- GACTCTAGAGGGCAATGAA-CAAAGTTCCAA-3′). The 35S promoter in PBI121 was replaced by the amplified 3 kb 2A11 and 2.5 kb TFM7 promoter fragments, respectively, by PCR using primers introducing two unique restriction sites (*Hin*dIII and *Xba*I) at the product ends. To construct *HP1* fruit-specific RNAi vectors, sequences from *HP1* cDNA (accession number AY531660) were isolated by RT-PCR using primers HP1-UF (5′-GCTCTCGAGCCTCTAGAGATCTGAAAAACG-3′), HP1-UR (5′-GCGAAGCTTGGCCTATCGGAGGCAGCAA-3′), HP1-DF (5′- CGAGAGCTCCAGTCGGCTACTCGGTCAAT-3′) and HP1-DR (5′- CGAGAATTCTTGGCCTATCGGAGGCAGCAA-3′). An inverted-repeat fragment of *hp1* was inserted downstream of the two fruit-specific promoters at the *Xba*I and *Sac*I restriction sites of the modified PBI121. The constructs 2A11-HP1-RNAi and TFM7-HP1-RNAi were thus generated.

The complete open reading frame (ORF) of *Cul4* was amplified by using primers CUL4YFP-F (5′-ACGCGTATGAAGAAAGCTAAGTCACAAGC-3′) and CUL4YFP-R (5′-GGATCCAGCAAGGTAGTTGTATATTTGAG-3′), incorporating restriction sites *Mlu*I and *Bam*HI at the product ends. The amplified fragment was cloned into the binary vector YFP-pBA002 (Hare *et al.*, 2003), and a fusion protein construct 35S-CUL4-YFP was generated. Similarly, the *HP1* ORF was amplified using primers HP1YFP-F (5′-CCTAGGAATGAGTGTATGGAACTACGTGG-3′) and HP1YFP-R (5′-GACGTCATGCAACCTTGTCAACTCT-

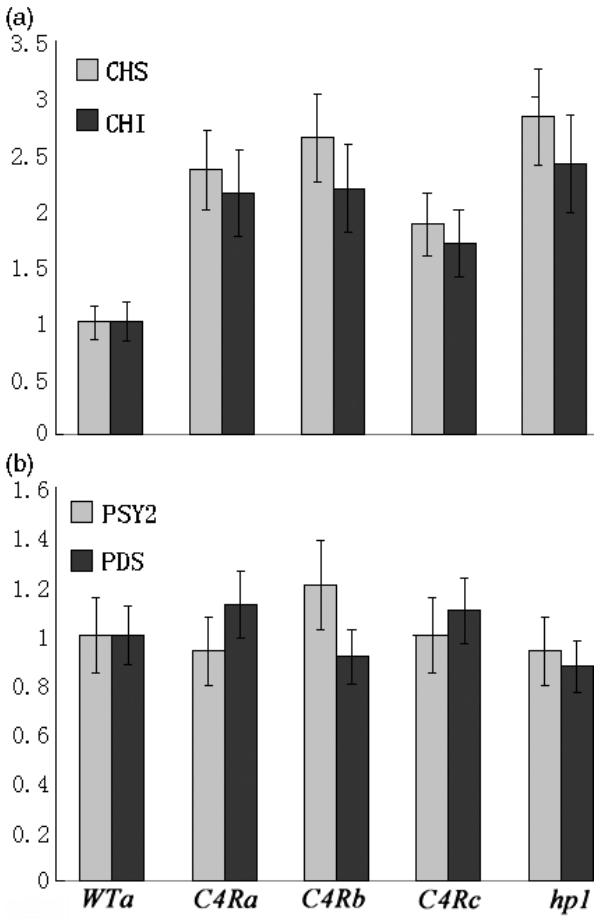

Figure 8. Real-time quantitative RT-PCR analysis of mRNA levels of anthocyanin and carotenoid biosynthetic pathway genes in fully expanded leaves from 40-day-old wild-type Ailsa Craig (*WTa*), three independent CUL4-deficient lines (*C4Ra, b* and *c*) and the *hp1* mutant.
All plants were grown in the artificial climate incubator. CHI, chalcone isomerase; CHS, chalcone synthase; PSY2, phytoene synthase 2; PDS, phytoene desaturase. Each bar represents three repetitions from each RNA sample (derived from pools of three leaves per plant). Standard errors are shown in each case.

TC-3′), incorporating restriction sites *Aat*II and *Avr*II, respectively, and a fusion protein construct 35S-HP1-YFP was generated.

Transgenic plants were generated by *Agrobacterium tumefaciens*-mediated transformation according to the method described by Fillatti *et al.* (1987), and transformed lines were first selected for kanamycin (70 mg l^{-1}) resistance and then analyzed by PCR to determine the presence of T-DNA. The primers designed to the *NPTII* (Kan^r) marker of PBI121 for confirmation of integration were 5′-GGCAATTACCTTATCCGCAA-3′ and 5′-AGAACTCGTCAAGAAGGCGA-3′.

Molecular analyses

Total RNAs were extracted using Trizol reagent according to the protocol provided by the manufacturer (Invitrogen, http://www.invitrogen.com/), and treated with DNaseI (TaKaRa; http://www.takara-bio.com). For semi-quantitative RT-PCR, the internal reference *UBI3* (GenBank accession no. X58253) was co-amplified with the target gene in every PCR reaction. Forward and reverse primers for RT-PCR analysis were designed for *UBI3* (forward, 5′-AGAAGAAGACCTACACCAAGCC-3′; reverse, 5′-TCCCAAGGGTTGTCACATACATC-3′), *CHS* (forward, 5′-AAGGATGTTCCTGGGCTTATCTC-3′; reverse, 5′-TTTTAGAGGCCCACAATGTAAGC-3′) and *CAB* (forward, 5′-CCAAGAACCGTGAACTCGAGGTG-3′; reverse, 5′-TACTGGGTCTGCAAGGTGATCAG-3′).

Primers for real-time RT-PCR were designed for *CUL4* (REALCUL4-F, 5′-GGAGGAATTGGAGGGGACATTA-3′; REALCUL4-R, 5′-GAAATCATGGACTTTTCAGCATCA-3′), *HP1* (REALHP1-F, 5′-CCGAGAATTGCAGACAGAATGT-3′; REALHP1-R, 5′-CCCTCTTCATGCTTGAAAATCA-3′), *CHS* (CHSreal-F, 5′-AGCCTGAGAAACTTAGGGCTAC-3′ CHSreal-R, 5′-CATTCAAGCCCTTCACCAGTAG-3′), *CHI* (CHIreal-F, 5′-TCAAGGCTTCCAGGATATGTCC-3′ CHIreal-R, 5′-GGATGTCCCGAACTTCTCCTTG-3′), *PSY2* (PSY2real-F, 5′-AGGGTGACCGATAAATGGAGAA-3′ PSY2real-R, 5′-CAAGACCAAAGATGCCCATACC-3′), *PDS* (PDSreal-F, 5′-TCGGAAGCAAGCGTAGTTTAGC-3′ PDSreal-R, 5′-GGAGCTTTCCTAACATTTCTCCT-3′) and the control *UBI3* (REALUBI3-F, 5′-AGGTTGATGACACTGGAAAGGTT-3′; REALUBI3-R, 5′-AATCGCCTCCAGCCTTGTTGTA-3′). The real-time PCR was performed according to the manufacturer's instructions (TaKaRa). Each sample was amplified in triplicate and all PCR reactions were performed on the iCycler® PCR system (Bio-Rad, http://www.bio-rad.com/). The tomato *ubi3* gene (accession number X58253) was used as a reference. REST software (Pfaffl *et al.*, 2002) was used to quantify the *Cul4* and *HP1* mRNA levels, with *ubi3* normalization by the $2^{-\Delta\Delta C_t}$ method. To confirm the specificity of the PCR reaction, PCR products were electrophoresed on a 1% agarose gel to verify accurate amplification product size.

Anthocyanin and chlorophyll assays

Chlorophyll and anthocyanins were extracted from fully expanded leaves of 30-day-old tomato plants and assayed according to the procedures described previously (Liu *et al.*, 2004 and Mustilli *et al.*, 1999, respectively).

Carotenoid extraction and analysis by HPLC

Carotenoid analysis was carried out according to previously described methods (Ronen *et al.*, 2000). The extracted carotenoids were separated by reverse-phase HPLC (HITACHI L-2000; http://www.hitachi-hta.com), and identified by their characteristic absorption spectra and their typical retention time, which corresponded to standards for lycopene and β-carotene. Peak areas were integrated using the chromatography software EZChrom Elite for Hitachi, version 3.1.5a (HITACHI).

Microscopy

Roots cut from 35S-CUL4-YFP, 35S-HP1-YFP and 35S-YFP transgenic tomato callus as well as non-transgenic wild-type callus (30 days old) were mounted on slides with gentle tapping and observed using differential interference contrast (DIC) optics on a Leica DMI6000B microscope (http://www.leica-microsystems.com). To observe yellow fluorescent protein (YFP), excitation was at 514 nm, and the spectral detector was set between 520 and 550 nm. Laser intensity was set at 50%, and exposure times were shorter than 1 sec.

Measurement of trichome density, floral and fruit size

Young leaves from *hp1*, CUL4-deficient and wild-type control plants were taken from 30-day-old plants grown in the artificial climate

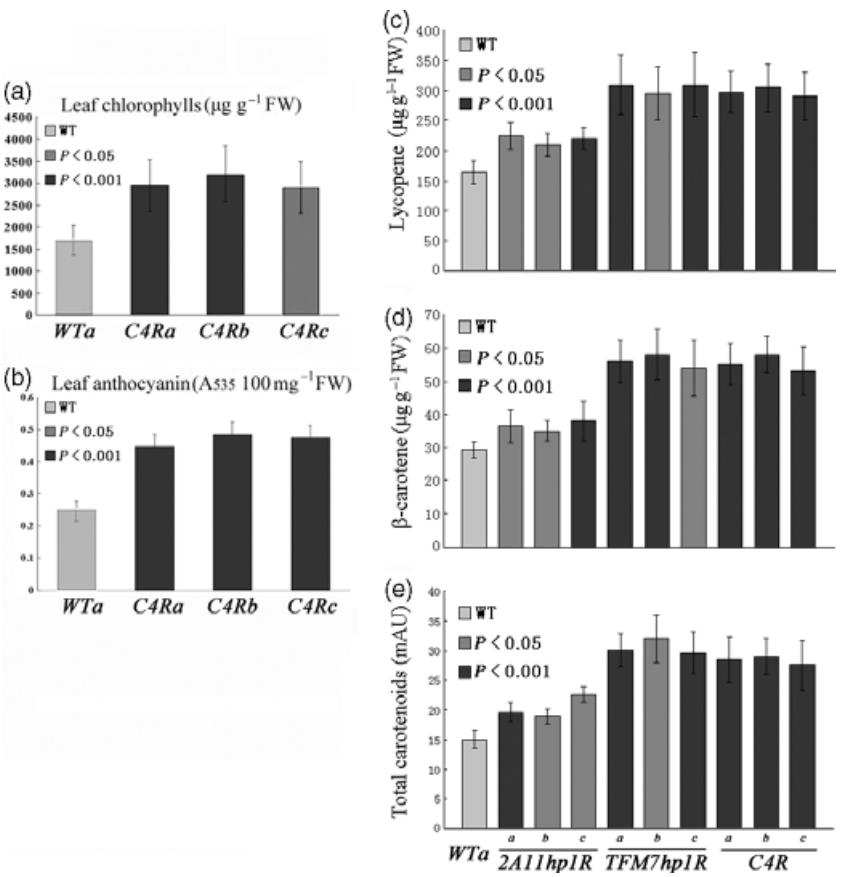

Figure 9. Quantification of flavonoid and carotenoid contents.
(a, b) Comparison of the leaf chlorophyll (a) and anthocyanin (b) contents between wild-type Ailsa Craig (*WTa*) and three independent CUL4-deficient lines (*C4Ra, b* and *c*). Mean values from 15 fully expanded leaves derived from each line and standard errors are shown. (c–e) Comparison of the lycopene (c), β-carotene (d) and total carotenoid (e) content of ripe fruits from wild-type Ailsa Craig (*WTa*), three independent CUL4-deficient lines (*C4Ra, b* and *c*) and three independent transgenic lines containing the fruit-specific promoters 2A11 (*2A11hp1Ra, b* and *c*) or TFM7 (*TFM7hp1Ra, b* and *c*). Mean values were calculated from measurements for three to four fruits taken from three sibling T_1 generation plants per line. Standard errors are shown. Statistical analysis of the differences in transgenic lines with respect to wild-type (*WTa*) was performed using Student's *t*-test.

incubator, and the trichome number was counted visually under a dissecting microscope (Leica). Leaf tracings were scanned and digitized for area determination using the graphic analysis program LeicaQWin. Trichome density was calculated as the trichome number per disc divided by the disc area. Size parameters were obtained by measuring the flowers at anthesis and red ripe fruits.

Determination of plastid compartment size in intact cells

Plastid compartment size was determined by counting plastid number and measuring plastid size in intact fixed separated cells, using previously described methods (Cookson *et al.*, 2003). The numbers of chloroplasts and chromoplasts in leaf mesophyll cells and/or fruit pericarp cells were determined using differential interference contrast (DIC) optics on a Leica DMI6000B microscope. Plan areas of individual cells and plastids within them were measured using the image analysis software LeicaQWin. The total plastid area was expressed as the product of the mean plastid area per cell and the plastid number per cell. A cell index parameter was calculated as a measure of the total plastid compartment size in relation to cell size, and was calculated as total plastid area per cell/cell plan area.

Yeast two-hybrid assays

Yeast two-hybrid assays were performed according to the *MATCHMAKER GAL4 Two-Hybrid System 3 User Manual* (Clontech, http://www.clontech.com/). Full-length open reading frame (ORF) cDNA sequences of tomato *Cul4*, *HP1* and *HP2* were cloned into the bait plasmid pGBKT7 (Clontech) and the prey plasmid pGADT7 (Cloentech), respectively, and fused with DNA-binding domain (BD) and activation domain (AD) sequences of yeast *GAL4* gene by PCR using primers CUL4TH-F1 (5′-GAATTCATGAAGAAAGCTAAGTCACAAGC-3′), CUL4TH-R1 (5′-GGATCCTAAGCAAGGTAGTTGTATATTTG-3′), HP1EYEF1 (5′-GAATTCATGAGTGTATGGAACTACGTG-3′), HP1EYER1 (5′-GTCGACCTAATGCAACCTTGTCAACTC-3′), HPEYEF1 (5′-CCATGGCTATGTTCAAAACTAACAATGTTAC-3′) and HP2EYER1 (5′-GGATCCTTATCGACGAAAATGGATATT-3′). The recombined bait plasmids and prey plasmids were co-transformed into yeast cells using LiAc-mediated yeast transformation. Photographs of resulting yeast colonies were taken 4 days after transfer. α-galactosidase quantitative assays were carried out according to the *Yeast Protocols Handbook* PT3024-1 (Clontech).

Acknowledgements

We thank Professor Nam-Hai Chua of Rockefeller University (New York) for providing us with YFP-pBA002. This work was supported by the Natural Science Foundation of China (grant no. 90717110), the National High Technology Research and Development Program of China (863 Program) (grant no. 2007AA10Z100), and the Research Fund for the Doctoral Program of Higher Education from the Chinese Ministry of Education (grant no. 20060610017).

Supplementary Material

The following supplementary material is available for this article online:
Figure S1. Predicted amino acid sequence alignments of tomato Cul4 (EU218537) and other Cul4 genes from *Schizosaccharomyces*

pombe (NM_001019619), *Caenorhabditis elegans* (NM_063124), *Drosophila melanogaster* (NM_136508), *Mus musculus* (BC010211), *Homo sapiens* (AF077188) and *Arabidopsis thaliana* (NM_123990).

This material is available as part of the online article from http://www.blackwell-synergy.com.

Please note: Blackwell publishing are not responsible for the content or functionality of any supplementary materials supplied by the authors. Any queries (other than missing material) should be directed to the corresponding author for the article.

References

Al Khateeb, W.M. and Schroeder, D.F. (2007) DDB2, DDB1A and DET1 exhibit complex interactions during Arabidopsis development. *Genetics*, **176**, 231–242.

Angers, S., Li, T., Yi, X., MacCoss, M.J., Moon, R.T. and Zheng, N. (2006) Molecular architecture and assembly of the DDB1–CUL4A ubiquitin ligase machinery. *Nature*, **443**, 590–593.

Bendich, A. (1991) Beta-carotene and immune response. *Proc. Nutr. Soc.* **50**, 263–274.

Bernhardt, A., Lechner, E., Hano, P. *et al.* (2006) CUL4 associates with DDB1 and DET1 and its downregulation affects diverse aspects of development in *Arabidopsis thaliana*. *Plant J.* **47**, 591–603.

Cang, Y., Zhang, J., Nicholas, S.A., Bastien, J., Li, B., Zhou, P. and Goff, S.P. (2006) Deletion of DDB1 in mouse brain and lens leads to p53-dependent elimination of proliferating cells. *Cell*, **127**, 929–940.

Castellano, M., Boniotti, M.B., Caro, E., Schnittger, A. and Gutierrez, C. (2004) DNA replication licensing affects cell proliferation or endoreplication in a cell type-specific manner. *Plant Cell*, **16**, 2380–2393.

Chen, X., Zhang, Y., Douglas, L. and Zhou, P. (2001) UV-damaged DNA-binding proteins are targets of CUL4a mediated ubiquitination and degradation. *J. Biol. Chem.* **276**, 48175–48182.

Chen, H., Shen, Y., Tan, X. *et al.* (2006) *Arabidopsis* CULLIN4 forms an E3 ubiquitin ligase with RBX1 and the CDD complex in mediating light control of development. *Plant Cell*, **18**, 1991–2004.

Cookson, P.J., Kiano, J.W., Shipton, C.A., Fraser, P.D., Romer, S., Schuch, W., Bramley, P.M. and Pyke, K.A. (2003) Increases in cell elongation, plastid compartment size and phytoene synthase activity underlie the phenotype of the *high pigment-1* mutant of tomato. *Planta*, **217**, 896–903.

Davuluri, G.R., van Tuinen, A., Mustilli, A.C. *et al.* (2004) Manipulation of DET1 expression in tomato results in photomorphogenic phenotypes caused by post-transcriptional gene silencing. *Plant J.* **40**, 344–354.

Davuluri, G.R., van Tuinen, A., Fraser, P.D. *et al.* (2005) Fruit-specific RNAi-mediated suppression of *DET1* enhances carotenoid and flavonoid content in tomatoes. *Nat. Biotechnol.* **23**, 890–895.

Figueroa, P., Gusmaroli, G., Serino, G. *et al.* (2005) Arabidopsis has two redundant Cullin3 proteins that are essential for embryo development and that interact with RBX1 and BTB proteins to form multisubunit E3 ubiquitin ligase complexes in vivo. *Plant Cell*, **17**, 1180–1195.

Fillatti, J.J., Kiser, J., Rose, R. and Comai, L. (1987) Efficient transfer of a glyphosate tolerance gene into tomato using a binary *Agrobacterium tumefaciens* vector. *BioTechnology*, **5**, 726–730.

Galpaz, N., Wang, Q., Menda, N., Zamir, D. and Hirschberg, J. (2008) Abscisic acid deficiency in the tomato mutant *high-pigment 3* leading to increased plastid number and higher fruit lycopene content. *Plant J.* **53**, 717–730.

Guo, H.S., Fei, J.F., Xie, Q. and Chua, N.H. (2003) A chemical-regulated inducible RNAi system in plants. *Plant J.* **34**, 383–392.

Hare, P.D., Møller, S.G., Huang, L.F. and Chua, N.H. (2003) LAF3, a novel factor required for normal phytochrome A signaling. *Plant Physiol.* **133**, 1592–1604.

Higa, L.A., Mihaylov, I.S., Banks, D.P., Zheng, J. and Zhang, H. (2003) Radiation-mediated proteolysis of CDT1 by CUL4–ROC1 and CSN complexes constitutes a new checkpoint. *Nat. Cell Biol.* **5**, 1008–1015.

Hu, J., McCall, C.M., Ohta, T. and Xiong, Y. (2004) Targeted ubiquitination of CDT1 by the DDB1–CUL4A–ROC1 ligase in response to DNA damage. *Nat. Cell Biol.* **6**, 1003–1009.

Hwang, E.S. and Bowen, P.E. (2002) Can the consumption of tomatoes or lycopene reduce cancer risk? *Integr. Cancer Ther.* **1**, 121–132.

Ishibashi, T., Kimura, S., Yamamoto, T., Furukawa, T., Takata, K., Uchiyama, Y., Hashimoto, J. and Sakaguchi, K. (2003) Rice UV-damaged DNA binding protein homologues are most abundant in proliferating tissues. *Gene*, **308**, 79–87.

Jin, J., Arias, E.E., Chen, J., Harper, J.W. and Walter, J.C. (2006) A family of diverse Cul4–Ddb1-interacting proteins includes Cdt2, which is required for S phase destruction of the replication factor Cdt1. *Mol. Cell*, **23**, 709–721.

Jones, B., Frasse, P., Olmos, E., Zegzouti, H., Li, Z.G., Latché, A., Pech, J.C. and Bouzayen, M. (2002) Down-regulation of DR12, an auxin-response-factor homolog, in the tomato results in a pleiotropic phenotype including dark green and blotchy ripening fruit. *Plant J.* **32**, 603–613.

Kendrick, R.E., Kerckhoffs, L.H.J., van Tuinen, A. and Koornneef, M. (1997) Photomorphogenic mutants of tomato. *Plant Cell Environ.* **20**, 746–751.

Kolotilin, I., Koltai, H., Tadmor, Y., Bar-Or, C., Reuveni, M., Meir, A., Nahon, S., Shlomo, H., Chen, L. and Levin, I. (2007) Transcriptional profiling of high pigment-2 (dg) tomato mutant links early fruit plastid biogenesis with its overproduction of phytonutrients. *Plant Physiol.* **145**, 389–401.

Li, B., Ruiz, J.C. and Chun, K.T. (2002) CUL-4A is critical for early embryonic development. *Mol. Cell. Biol.* **22**, 4997–5005.

Li, T., Chen, X., Garbutt, K.C., Zhou, P. and Zheng, N. (2006) Structure of DDB1 in complex with a paramyxovirus V protein: viral hijack of a propeller cluster in ubiquitin ligase. *Cell*, **124**, 105–117.

Lieberman, M., Segev, O., Gilboa, N., Lalazar, A. and Levin, I. (2004) The tomato homolog of the gene encoding UV DAMAGED DNA BINDING protein 1 (DDB1) underlined as the gene that causes the *high pigment-1* mutant phenotype. *Theor. Appl. Genet.* **108**, 1574–1581.

Liu, Y., Roof, S., Ye, Z., Barry, C., van Tuinen, A., Vrebalov, J., Bowler, C. and Giovannoni, J. (2004) Manipulation of light signal transduction as a means of modifying fruit nutritional quality in tomato. *Proc. Natl Acad. Sci. USA*, **101**, 9897–9902.

Maple, J. and Møller, S.G. (2007) Plastid division: evolution, mechanism and complexity. *Ann. Bot.* **99**, 565–579.

Mustilli, A.C., Fenzi, F., Ciliento, R., Alfano, F. and Bowler, C. (1999) Phenotype of the tomato high pigment-2 mutant is caused by a mutation in the tomato homolog of DEETIOLATED1. *Plant Cell*, **11**, 145–157.

Osaka, F., Saeki, M., Katayama, S. *et al.* (2000) Covalent modifier NEDD8 is essential for SCF ubiquitin-ligase in fission yeast. *EMBO J.* **19**, 3475–3484.

Pear, J.R., Ridge, N., Rasmussen, R., Rose, R.E. and Houck, C.M. (1989) Isolation and characterization of a fruit-specific cDNA and the corresponding genomic clone from tomato. *Plant Mol. Biol.* **13**, 639–651.

Pepper, A., Delaney, T., Washburn, T., Poole, D. and Chory, J. (1994) *DET1*, a negative regulator of light-mediated development and

gene expression in *Arabidopsis*, encodes a novel nuclear-localized protein. *Cell*, **78**, 109–116.

Peters, J.L., Szell, M. and Kendrick, R.E. (1998) The expression of light-regulated genes in the high-pigment-1 mutant of tomato. *Plant Physiol.* **117**, 797–807.

Petroski, M.D. and Deshaies, R.J. (2005) Function and regulation of cullin-RING ubiquitin ligases. *Nat. Rev. Mol. Cell Biol.* **6**, 9–20.

Pfaffl, M.W., Horgan, G.W. and Dempfle, L. (2002) Relative expression software tool (RESTa) for group-wise comparison and statistical analysis if relative expression results in real-time PCR. *Nucleic Acids Res.* **30**, e36.

Pintard, L., Willis, J.H., Willems, A. *et al.* (2003) The BTB protein MEL-26 is a substrate-specific adaptor of the CUL-3 ubiquitin-ligase. *Nature*, **425**, 311–316.

Raynaud, C., Perennes, C., Reuzeau, C., Catrice, O., Brown, S. and Bergounioux, C. (2005) Cell and plastid division are coordinated through the prereplication factor AtCDT1. *Proc. Natl Acad. Sci. USA*, **102**, 8216–8221.

Ronen, G., Carmel-Goren, L., Zamir, D. and Hirschberg, J. (2000) An alternative pathway to beta-carotene formation in plant chromoplasts discovered by map-based cloning of beta and old-gold color mutations in tomato. *Proc. Natl Acad. Sci. USA*, **97**, 11102–11107.

Sambrook, J. and Russell, W.R. (2001) *Molecular Cloning: A Laboratory Manual*, 3rd edn. Cold Spring Harbor, NY: Cold Spring Harbor Laboratory Press.

Santino, C.G., Stanford, G.L. and Conner, T.W. (1997) Developmental and transgenic analysis of two tomato fruit enhanced genes. *Plant Mol. Biol.* **33**, 405–416.

Schroeder, D.F., Gahrtz, M., Maxwell, B.B., Cook, R.K., Kan, J.M., Alonso, J.M., Ecker, J.R. and Chory, J. (2002) De-etiolated 1 and damaged DNA binding protein 1 interact to regulate Arabidopsis photomorphogenesis. *Curr. Biol.* **12**, 1462–1472.

Schwechheimer, C. and Villalobos, L.I. (2004) Cullin-containing E3 ubiquitin ligases in plant development. *Curr. Opin. Plant Biol.* **7**, 677–686.

Smalle, J. and Vierstra, R.D. (2004) The ubiquitin 26S proteasome proteolytic pathway. *Annu. Rev. Plant Biol.* **55**, 555–590.

Sun, N.K., Lu, H.P. and Chao, C.C. (2002) Identification of rat DDB1, a putative DNA repair protein, and functional correlation with its damaged-DNA recognition activity. *J. Biomed. Sci.* **9**, 371–380.

Wertz, I.E., O'Rourke, K.M., Zhang, Z., Dornan, D., Arnott, D., Deshaies, R.J. and Dixit, V.M. (2004) Human de-etiolated-1 regulates c-Jun by assembling a CUL4A ubiquitin ligase. *Science*, **303**, 1371–1374.

Yen, H.C., Shelton, B.A., Howard, L.R., Lee, S., Vrebalov, J. and Giovannoni, J.J. (1997) The tomato high-pigment (hp) locus maps to chromosome 2 and influences plastome copy number and fruit quality. *Theor. Appl. Genet.* **95**, 1069–1079.

Zhong, W., Feng, H., Santiago, F.E. and Kipreos, E.T. (2003) CUL-4 ubiquitin ligase maintains genome stability by restraining DNA replication licensing. *Nature*, **423**, 885–889.

The GenBank accession number for the tomato *Cul4* cDNA sequence is EU218537.

